

Color vision in an elderly patient with protanopic genotype and successfully treated unilateral age-related macular degeneration

Takaaki Kitakawa · Takaaki Hayashi ·
Satoshi Tsuzuranuki · Akiko Kubo ·
Hiroshi Tsuneoka

Received: 13 October 2010 / Accepted: 8 March 2011 / Published online: 11 November 2011
© Springer Science+Business Media B.V. 2011

Abstract We investigated differences in color discrimination between the fellow eye and the affected eye successfully treated for unilateral age-related macular degeneration (AMD) in a 69-year-old male patient with protanopia. His best-corrected visual acuity (BCVA) was 1.2 in the right eye (RE) and 0.2 in the left eye (LE). Fundus and angiographic findings showed classic choroidal neovascularization (CNV) secondary to AMD in the LE. BCVA of the LE improved to 0.4, and CNV resolved by 15 months after initiating combined anti-vascular endothelial growth factor and photodynamic therapies. After CNV closure, the Farnsworth dichotomous was performed, showing confusion patterns of the protan axis in either eye. The Farnsworth-Munsell 100-hue test showed a total error score of 520 in the LE, much higher than the score of 348 in the RE. Complete genotypes of the long-wavelength-sensitive (L-) cone and middle-wavelength-sensitive (M-) cone opsin genes were determined by polymerase chain reaction, revealing that the patient had a single 5' L-M 3' hybrid

gene (encoding an M-cone opsin), with this genotype responsible for protanopia (the L-cone opsin gene was non-functional), instead of the L-cone and M-cone opsin gene arrays. Poorer color vision discrimination in the LE than the RE remained present despite closure of CNV. The presence and type of congenital color vision defect can be confirmed using molecular genetic testing even if complications of acquired retinal diseases such as AMD are identified.

Keywords Age-related macular degeneration · Choroidal neovascularization · Color vision defects · Molecular genetics · Genetic analysis

Introduction

Age-related macular degeneration (AMD) is the leading cause of severe vision loss in older adults in developed countries. Recent studies have shown that the combination of anti-vascular endothelial growth factor (VEGF) therapy and photodynamic therapy (PDT) is effective against choroidal neovascularization (CNV) due to AMD [1]. Distance visual acuity assessment is the most commonly used method to evaluate visual function in AMD patients, and few reports have assessed color vision after treatment for AMD. This is due to the difficulty in adequately evaluating color discrimination in AMD patients

T. Kitakawa · T. Hayashi (✉) · S. Tsuzuranuki ·
H. Tsuneoka
Department of Ophthalmology, The Jikei University
School of Medicine, 3-25-8, Nishi-shimbashi, Minato-ku,
Tokyo 105-8461, Japan
e-mail: taka@jikei.ac.jp

A. Kubo
Department of Ophthalmology, Kinan Hospital, Mie,
Japan

≥65 years of age, particularly as such patients often have diabetes in addition to senile cataracts.

Congenital color vision defects such as X-linked recessively inherited and non-progressive disorders are common [2], with an incidence of approximately 8% in Caucasian men and 5% in Japanese men. The presence of congenital color vision defects cannot therefore be ignored for assessing color vision in AMD patients.

This report investigated differences in color discrimination between the fellow eye and the affected eye successfully treated for AMD in a male patient with protanopia (one type of dichromacy in congenital color vision defects) diagnosed by molecular genetic analysis.

Case report

This study was approved by the institutional review board of The Jikei University School of Medicine. The protocol adhered to the tenets of the Declaration of Helsinki, and informed consent was obtained from the patient.

A 69-year-old man became aware of distorted vision and loss of visual acuity in May 2007, and presented to our department on August 16, 2007. The patient had long history of smoking and a medical history of diabetes mellitus, hypertension, hyperlipidemia, arrhythmia and congenital color blindness. On initial evaluation, decimal best-corrected visual acuity (BCVA) was 1.2 in the right eye (RE) and 0.2 in the left eye (LE). No abnormalities were found except mild cataracts in the anterior segments and media of both eyes. Intraocular pressure was 13 mmHg bilaterally. Fundoscopy showed no notable abnormalities in the RE (Fig. 1a), but a subfoveal grayish-yellow lesion with subretinal hemorrhage in the LE (Fig. 1b). Fluorescein angiography of the LE showed hyperfluorescence in the foveal area due to leakage from predominantly classic CNV secondary to AMD (Fig. 1c). Indocyanine green angiography showed focal hyperfluorescence in the area corresponding to the CNV (Fig. 1d). Optical coherence tomography (OCT) (OCT3 Stratus; Carl Zeiss Meditec AG, Dublin, CA, USA) showed the appearance of the normal foveal depression in the RE (Fig. 1e), and confirmed the presence of subfoveal CNV in the LE (Fig. 1f). The patient underwent verteporfin (Visudyne®; Novartis AG, Bülach, Switzerland) PDT

2 weeks after the first visit. Three months later, combined therapy comprising verteporfin PDT and intravitreal injection of bevacizumab (Avastin®, 1.25 mg/0.05 ml; Genentech, South San Francisco, CA, USA), a non-selective VEGF inhibitor, was initiated to treat persistent CNV. At the 3-month follow-up, no persistent or recurrent CNV was identified on angiography or OCT. BCVA of the LE improved to 0.4 and CNV resolved (Fig. 1g) by 15 months after starting combined therapy. At this time, color vision was assessed monocularly using the Farnsworth Dichotomous Test (panel D-15) and the Farnsworth-Munsell 100-hue (F-M 100-hue) test. The result for panel D-15 showed confusion patterns of the protan axis in both LE (Fig. 2a) and RE (Fig. 2b). The F-M 100-hue test revealed a total error score (TES) of 520 in the LE (Fig. 2c), much higher than the score of 348 in the RE (Fig. 2d). Regarding orientation axes, the RE indicated a significant red–green axis, whereas the LE indicated both red–green and blue–yellow axes.

For molecular genetic analysis, genomic DNA was isolated from whole blood. Genotype of the long-wavelength-sensitive (L) cone and middle-wavelength-sensitive (M) cone opsin genes was completely determined by polymerase chain reaction and sequencing as previously reported [2–4]. In normal male trichromats, L- and M-opsin genes are arranged in a head-to-tandem array (Fig. 3) on the X chromosome, whereas this patient showed a single 5' L–M 3' hybrid gene (encoding an M opsin) (Fig. 3) with the genotype responsible for protanopia [2]. The L-opsin gene was thus non-functioning in this patient.

Discussion

Determining which type of congenital color vision defects is present in elderly patients is difficult using standard color vision tests alone, as aging, cataracts and age-related maculopathy all affect color discrimination. In fact, our patient had senile cataracts, diabetes and unilateral AMD in addition to congenital color vision defects.

Previous studies have shown that TES for the F-M 100 hue test is significantly higher in elderly subjects than in younger subjects [5, 6]. Diabetic patients with minimal or even no diabetic retinopathy also show significantly higher mean TES for the F-M 100 hue

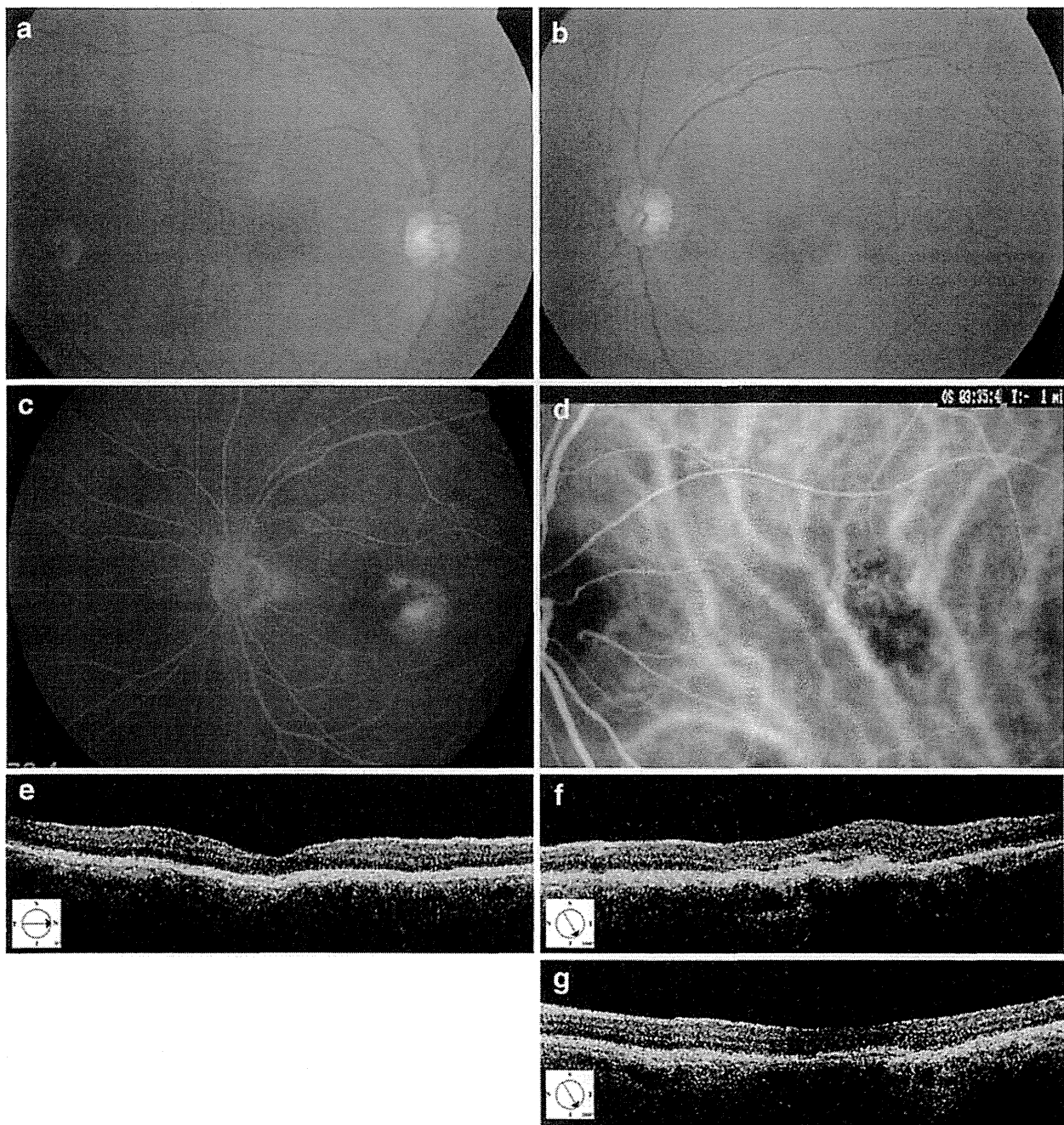


Fig. 1 Images from fundoscopy (**a**, **b**), mid-phase fluorescein angiography (FA) (**c**), mid-phase indocyanine green angiography (ICGA) (**d**) and optical coherence tomography (OCT) (**e**, **f**, **g**) in the patient. Fundoscopy shows no notable abnormalities in the right eye (**a**), but a subfoveal grayish-yellow lesion with subretinal hemorrhage in the left eye (**b**). FA of the left eye shows hyperfluorescence in the foveal area due to leakage from

predominantly classic choroidal neovascularization (CNV) (**c**). ICGA of the left eye shows focal hyperfluorescence in the area corresponding to the CNV (**d**). OCT shows the appearance of the normal foveal depression in the right eye (**e**), subfoveal CNV in the left eye (**f**), and the resolved CNV (**g**) in the left eye at 15 months after starting combined therapy

test than age-matched normal controls [7, 8]. Those studies have identified increased lens density, aging and diabetes as factors affecting color discrimination.

We have already identified genotype–phenotype correlations in male subjects with congenital color vision defects [2, 9]. In the present patient, the type of

Fig. 2 Results of the Farnsworth Dichotomous Test (Panel D-15) test (a, b), the Farnsworth-Munsell 100-hue (F-M 100-hue) test (c, d). Panel D-15 results show confusion patterns of the protan axis in the left (a) and right eyes (b). F-M 100-hue results show total error scores of 520 in the left eye (c) and 348 in the right eye (d)

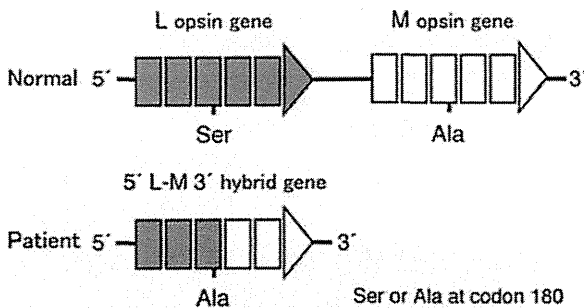
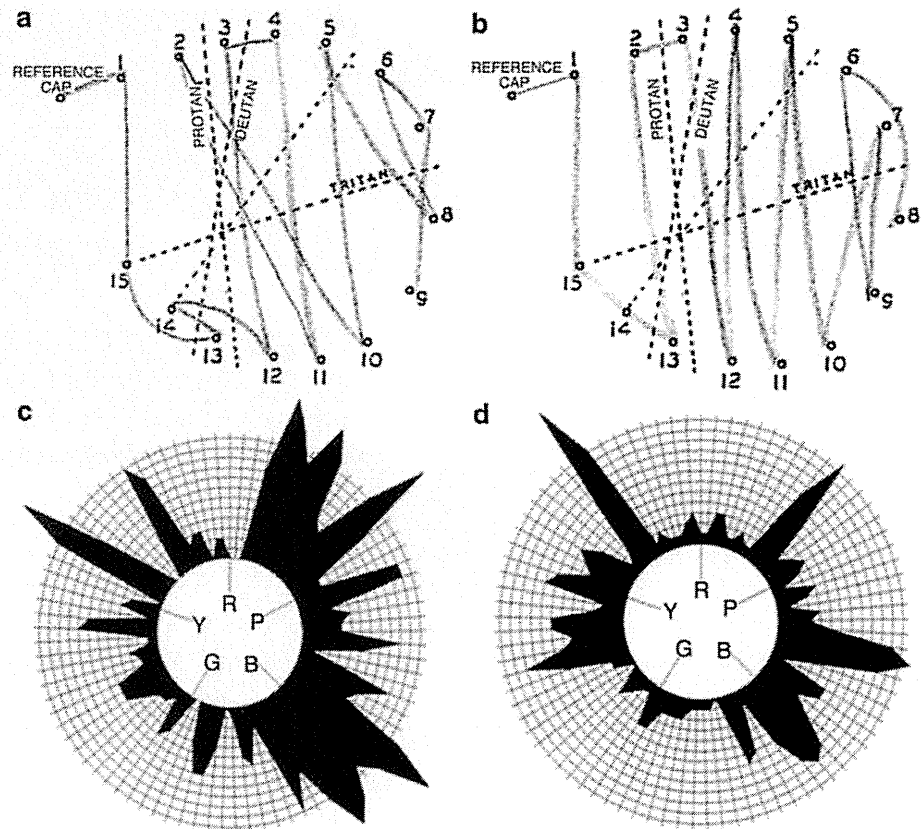


Fig. 3 Genotype of the L- and M-opsin gene array. In normal male trichromats (Normal), L- and M-opsin genes are arranged in a head-to-tandem array on the X chromosome, whereas this patient shows a single 5' L-M 3' hybrid gene (encoding an M opsin), with this genotype being responsible for protanopia

congenital color vision defects was diagnosed as protanopia by molecular genetic analysis (Fig. 3). When color discrimination was compared between the fellow eye and the affected eye, conditions (age, senile cataracts, diabetes and protanopia) were equivalent between eyes. Results of the F-M 100-hue test revealed poorer color discrimination in the LE (Fig. 2c) than in the RE (Fig. 2d). Differences in color discrimination between the eyes were attributed

to the resolved unilateral CNV confirmed by angiography and OCT. Poorer color discrimination in the LE than in the RE is thus likely to be due to loss of function of all three cone classes in the fovea.

In conclusion, poorer color discrimination in the LE than in the RE was due to AMD, for which complete closure of CNV was achieved. The presence and type of congenital color vision defect can be confirmed using molecular genetic testing even if complications of acquired retinal diseases such as AMD are present.

Acknowledgments This work was supported by grants from The Jikei University Research Fund (T.H.) and the Vehicle Racing Commemorative Foundation (T.H. and H.T.).

References

1. Dhalla MS, Shah GK, Blinder KJ, Ryan EH Jr, Mitra RA, Tewari A (2006) Combined photodynamic therapy with verteporfin and intravitreal bevacizumab for choroidal neovascularization in age-related macular degeneration. *Retina* 26:988–993. doi:10.1097/01.iae.0000247164.70376.91
2. Deeb SS, Hayashi T, Winderickx J, Yamaguchi T (2000) Molecular analysis of human red/green visual pigment gene

- locus: relationship to color vision. *Methods Enzymol* 316:651–670
3. Young TL, Deeb SS, Ronan SM et al (2004) X-linked high myopia associated with cone dysfunction. *Arch Ophthalmol* 122:897–908. doi:10.1001/archophth.122.6.897
 4. Hayashi T, Kubo A, Takeuchi T, Gekka T, Goto-Omoto S, Kitahara K (2006) Novel form of a single X-linked visual pigment gene in a unique dichromatic color-vision defect. *Vis Neurosci* 23:411–417. doi:10.1017/S0952523806233029
 5. Verriest G, Van Laethem J, Uvijls A (1982) A new assessment of the normal ranges of the Farnsworth-Munsell 100-hue test scores. *Am J Ophthalmol* 93:635–642
 6. Beirne RO, McIlreavy L, Zlatkova MB (2008) The effect of age-related lens yellowing on Farnsworth-Munsell 100 hue error score. *Ophthalmic Physiol Opt* 28:448–456. doi:10.1111/j.1475-1313.2008.00593.x
 7. Roy MS, Gunkel RD, Podgor MJ (1986) Color vision defects in early diabetic retinopathy. *Arch Ophthalmol* 104:225–228
 8. Hardy KJ, Lipton J, Scase MO, Foster DH, Scarpello JH (1992) Detection of colour vision abnormalities in uncomplicated type 1 diabetic patients with angiographically normal retinas. *Br J Ophthalmol* 76:461–464
 9. Jagla WM, Jagle H, Hayashi T, Sharpe LT, Deeb SS (2002) The molecular basis of dichromatic color vision in males with multiple red and green visual pigment genes. *Hum Mol Genet* 11:23–32

A novel mutation (Cys83Tyr) in the second zinc finger of *NR2E3* in enhanced S-cone syndrome

Amândio Rocha-Sousa · Takaaki Hayashi · Nuno Lourenço Gomes · Susana Penas · Elisete Brandão · Paulo Rocha · Mitsuyoshi Urashima · Hisashi Yamada · Hiroshi Tsunooka · Fernando Falcão-Reis

Received: 30 October 2009 / Revised: 25 July 2010 / Accepted: 26 July 2010 / Published online: 20 August 2010
© Springer-Verlag 2010

Abstract

Background Enhanced S-cone syndrome (ESCS) is an autosomal recessive retinal disorder characterized by an increased number of S-cones over L/M cones and rods. Mutations in the *NR2E3* gene, encoding a photoreceptor-specific nuclear receptor, are identified in patients with ESCS. The purpose of this study is to report the ophthalmic features of a 25-year-old Portuguese male with a typical ESCS phenotype and a novel homozygous *NR2E3* mutation.

Methods The patient underwent a detailed ophthalmic examination including fundus photography, fluorescein angiography (FAF), fundus autofluorescence imaging (FAI), and spectral domain optical coherence tomography (SD-OCT). Full-field electroretinography (ERG), S-cone ERG, and multifocal ERG were performed. Mutation screening of the *NR2E3* gene was performed with polymerase chain reaction amplification and direct sequencing.

Results The patient had poor visual acuity but good color vision. Funduscopy showed degenerative changes from the vascular arcades to the midperipheral retina. The SD-OCT revealed macular schisis and cystoid changes that had no fluorescein leakage. The posterior pole showed diffusely increased autofluorescence compared with eccentric areas in both eyes. International-standard full-field ERG showed the typical pathognomonic changes associated with ESCS and the short-wavelength flash ERG was simplified, delayed, and similar to the standard photopic flash ERG. Multifocal ERG showed widespread delay and reduction. Genetic analysis revealed a novel homozygous mutation (p.C83Y), which resides in the second zinc finger of the DNA-binding domain.

Conclusions This homozygous mutation is likely to affect binding to target DNA sites, resulting in a non-functional behavior of NR2E3 protein. It is associated

Presented at the EVER 2006 Meeting, Vilamoura, Portugal

A. Rocha-Sousa (✉) · N. L. Gomes · S. Penas · E. Brandão · P. Rocha · F. Falcão-Reis
Department of Ophthalmology, Hospital de São João, Porto, Portugal
e-mail: arsousa@med.up.pt

N. L. Gomes
e-mail: nunolgomes@gmail.com

S. Penas
e-mail: spenas75@yahoo.com

E. Brandão
e-mail: elisetebrandao@netcabo.pt

P. Rocha
e-mail: prochax@gmail.com

F. Falcão-Reis
e-mail: falcaor@med.up.pt

A. Rocha-Sousa
Physiology Department, Faculty of Medicine, University of Porto, Porto, Portugal

T. Hayashi · H. Tsunooka
Department of Ophthalmology,
The Jikei University School of Medicine,
Tokyo, Japan

T. Hayashi
e-mail: takaaki@amy.hi-ho.nc.jp

M. Urashima
Division of Molecular Epidemiology,
The Jikei University School of Medicine,
Tokyo, Japan
e-mail: urashima@jikei.ac.jp

H. Yamada
Department of Molecular Genetics, Institute of DNA Medicine,
The Jikei University School of Medicine,
Tokyo, Japan
e-mail: hyamad@jikei.ac.jp

with a typical form of ESCS with a nondetectable rod response and reduced/delayed mfERG responses at all eccentricities.

Keywords Enhanced S-cone syndrome, NR2E3 · S-cone · Retina · ERG

Introduction

Most retinal dystrophies are the result of either a generalized rod dysfunction, a generalized cone dysfunction (involving all three cone subtypes), or a generalized dysfunction of both rods and cones either simultaneously or successively. In 1990, Marmor [1] described a series of eight patients with night blindness, cystoid maculopathy, degenerative changes in the region of the vascular arcades, and loss of visual field. These patients showed S-cone hypersensitivity in electrophysiological testing; this condition was designated enhanced S-cone syndrome (ESCS). The ESCS has an autosomal recessive inheritance pattern and is characterized by hypersensitivity to short wavelength flashes with a concomitant decreased rod and L and M cone response [1–3].

Over ten mutations of the *NR2E3* gene have been identified in European patients with ESCS [4]. This gene encodes a photoreceptor-specific nuclear receptor. It consists of eight exons mapped on chromosome 15q24 [5]. Functionally, *NR2E3* protein regulates the proper differentiation and maturation of rod and cone photoreceptors [6–10]. To date, more than 30 mutations in the *NR2E3* gene have been described not only in ESCS [4, 11–15] but also in Goldman–Favre syndrome (GFS) [11, 16], autosomal recessive retinitis pigmentosa [17, 18], autosomal dominant retinitis pigmentosa [17, 19], and clumped pigmentary retinal degeneration [11]. Because appropriate ERG analyses demonstrated a relatively enhanced S-cone function and the presence of *NR2E3* mutations in GFS, it was concluded that the two diseases are likely to be one clinical entity, being the GFS the severe phenotype [11, 16, 20].

Although characteristic electroretinographic responses are usually essential for diagnosis, there is a variable spectrum of disease severity in patients with ESCS. We describe the clinical findings of a Portuguese patient with ESCS with a novel homozygous mutation in the *NR2E3* gene and exhibited a typical phenotype.

Materials and methods

Clinical studies

Ophthalmic examination included best-corrected visual acuity (BCVA), slit-lamp and dilated fundus observation,

Goldmann kinetic perimetry, chromatic vision testing, fluorescein angiogram (FAF), fundus autofluorescence imaging (FAI), spectral domain optical coherence tomography (SD-OCT), contrast sensitivity, dark adaptometry, and electrophysiological testing. Color vision testing included color contrast sensitivity threshold and the Farnsworth 100-hue test. The color contrast sensitivity thresholds were measured as proposed by Arden et al. (1988). In brief, the system uses a calibrated 21-inch color monitor to present random letters as targets to be identified. The letters are of equal luminance to the background, and can only be recognized because their hue differs from the background. All stimuli are equiluminant with the background. This is ensured by a preliminary adjustment (in every patient) of the relative luminance of the red and green and green and blue phosphors. Then a modified binary search is carried out to determine the threshold color contrast along the protan, deutan, and tritan color confusion lines [21]. All these color vision tests were performed monocularly. Cross-sectional retinal images were evaluated using SD-OCT (SPECTRALIS Spectral-domain OCT, Heidelberg Engineering, Heidelberg, Germany). The SD-OCT was taken horizontally through the fovea (transverse width of 20°). Dark adaptometry was performed based on the Goldman–Wecker adaptometer. Briefly, the patient was pre-adapted under photopic conditions (30 cd/m²) for 5 min. The dark adaptation characteristic was then assessed by measuring detection thresholds under scotopic conditions over a 30-min period.

Electrophysiological evaluation included full-field electroretinograms (ERG) using a Ganzfeld dome, long duration ON-OFF ERG, S-cone ERG, Electro-oculogram (EOG), and multifocal ERG (mf ERG). The ERG testing was performed according to the protocol of the International Society for Clinical Electrophysiology of Vision [22]. Briefly, under dilation and after dark adaptation (30 min), a dim white flash of 0.01–0.05 cd·s/m² was used for the scotopic (rod) response and a single white bright-flash (3 cd·s/m²) for the combined response. After light adaptation (10 min; 25 cd/m²), a brief white flash (3 cd·s/m²) was superimposed for the photopic response. The 30-Hz ERG was obtained in the same conditions using a 30-Hz flickering stimulation. The S-cone ERG was performed, under photopic conditions, using a blue stimulus (440 nm; 10 ms; 65 cd/m²) on an orange (660 nm; 350 cd/m²) background [23, 24]. For the L/M cones ON-OFF ERG, the 200-ms orange (660 nm; 350 cd/m²) stimulus was used on a green (530 nm; 130 cd/m²) background [25]. The EOG was obtained after a room light pre-adaptation period of 10 min [26]. Acquisitions were made after 15 min of dark adaptation and repeated after 15 min of light adaptation. The mfERG was acquired using an array of 61 stimulus (200 cd/m²) according to the recommendations of ISCEV [27]. All the electrophysiological exams were performed using the Metrovision

vision monitor (Pérenchies, France). For the ON-OFF ERG and the S-cone ERG, an additional external led stimulator was used (CH electronics).

Molecular genetic studies

The protocol adhered to the Declaration of Helsinki, and informed consent was obtained from the participant. Genetic analysis was performed at the Department of Ophthalmology at The Jikei University as previously described [12, 15]. Briefly, genomic DNA was extracted from venous blood samples using a Puregene Blood DNA Isolation kit (Gentra Systems, Minneapolis, MN). For mutation screening, all exons (exon 1 to exon 8) and the promoter region of the *NR2E3* gene were amplified by polymerase chain reaction (PCR) using previously reported primers [12, 15]. The PCR products were purified with a QIAquick PCR Purification kit (Qiagen, Tokyo, Japan) and

used as the template for sequencing. Both strands were sequenced on an automated sequencer (3730xl DNA Analyzer, Applied Biosystems, Foster City, CA) using a BigDye Terminator kit V3.1 (Applied Biosystems). A nucleotide variation in exon 3 was analyzed in 100 normal controls without any retinal diseases.

Results

Clinical findings

A 25-year-old male patient was referred to our hospital with suspected X-linked juvenile retinoschisis. The patient was one of the three children from a consanguineous couple (second-degree cousins) and was the only family member with visual symptoms. His chief complaint was of decreased vision but, even after inquiry, he denied nyctopia. His BCVA was 0.5 in

Fig. 1 Fundus photographs and fluorescein angiograms (FAF) images. Color fundus montages of the right eye (a) and left eye (b) show degenerative lesions in the midzonal retinal areas, near the arcades with nummular pigmentary changes at the RPE level. Absence of foveal reflex and the presence of schisis-like changes in both maculae are also observed. Midphase fluorescein angiograms of the right eye (c) and left eye (d) show no leakage in the maculas. The fundus autofluorescence images (e and f) show a diffusely increased autofluorescence (AF) associated with the arcades with some sparing of central and inferior macular area. The SD-OCT images show the presence of macular schisis with cystoid changes in the right (g) and left maculas (h) in the inner and outer nuclear layers

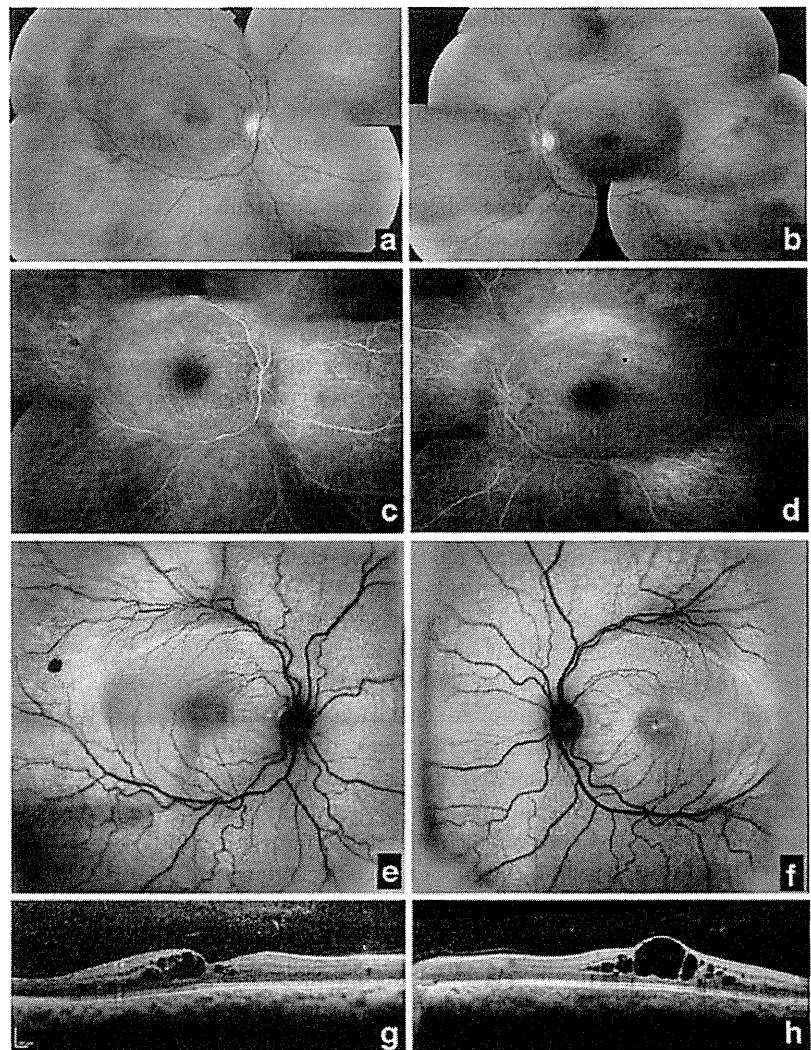
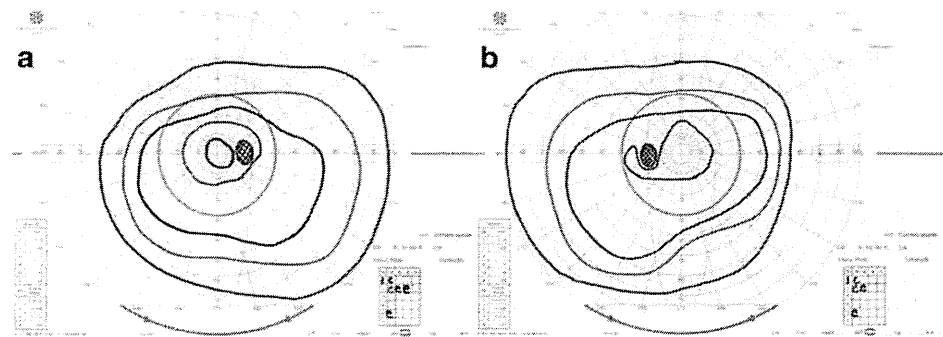


Fig. 2 Goldmann perimetry shows decreased central sensitivity with constriction of the I/2e and/or I/3e isopters (a I/2e: 10° of fixation in the right and b I/3e: 20° of fixation in the left), but normal peripheral visual fields



the right eye and 0.25 in the left eye. The anterior segment examination was unremarkable. Intraocular pressure was within the normal range. Fundoscopy showed bilateral foveal schisis-like changes (Fig. 1a, b). In addition, nummular pigmentary deposits were observed at the RPE level in the mid-periphery and along the vascular arcades, without vascular attenuation. FAF did not reveal any hyperfluorescence or leakage at the macular lesions (Fig. 1c, d). FAI showed diffusely increased AF over broad, crescent-like areas associated with the vascular arcades and optic disc in both eyes. More eccentric areas were hypofluorescent in comparison. Parafoveal hyperfluorescence was greater in the left eye compared to the right eye (Fig. 1e, f). The SD-OCT images confirmed the presence of macular schisis with cystoid changes in both maculae (Fig. 1g, h).

Functional evaluation

Color vision testing did not demonstrate a preferred axis of chromatic confusion, with 100 and 186 error scores in the right and left eye respectively on the Farnsworth 100-hue. The CCS thresholds were within normal limits. Goldmann perimetry revealed bilaterally decreased central sensitivity with constriction of the I/2e and/or I/3e isopters (I/3e: 20° of fixation in the left and I/2e: 10° of fixation in the right). However, there was no constriction of the visual fields (Fig. 2). The dark adaptometry curve showed a monophasic pattern with elevated cone threshold without the characteristic decrease that is attributed to rod function in normal individuals (Fig. 3).

Electrodiagnostic tests revealed characteristic patterns for ESCS. Scotopic dim flash rod ERG were undetectable. The waveforms of combined (rod-plus-cone) responses were similar to those of the photopic responses. Flicker ERGs of 30-Hz were smaller than the single flash cone a-waves (Fig. 4). The ERG results of specific chromatic stimulation showed that most of the ERG responses were arising from S-cone systems. S-cone ERG were delayed, simplified, and resemble the single flash cone ERG (Fig. 5). The ON-OFF responses with 200-ms orange stimulation, which are originated from the L/M cones [23], were markedly decreased in the patient, indicating minimal

responses to L/M cone stimulation (Fig. 5). The OFF L/M cones response was absent.

The EOG light rise was detected, with a reduction on the Arden index (1.56 and 1.65, for a normal value of 1.85).

Comparing the mfERG to the mfERG of normal subjects, reduced amplitudes and delayed implicit times, of both N1 and P1 components, were observed at all eccentricities and at all retinal locations (Fig. 6).

Molecular genetic findings

The genetic analysis identified a novel homozygous mutation in exon 3. This mutation leads to the substitution of an adenine for a guanine base (c.248G>A). At the proteic level, this causes the substitution of a tyrosine for a cysteine at position 83 on the highly conserved DNA-binding

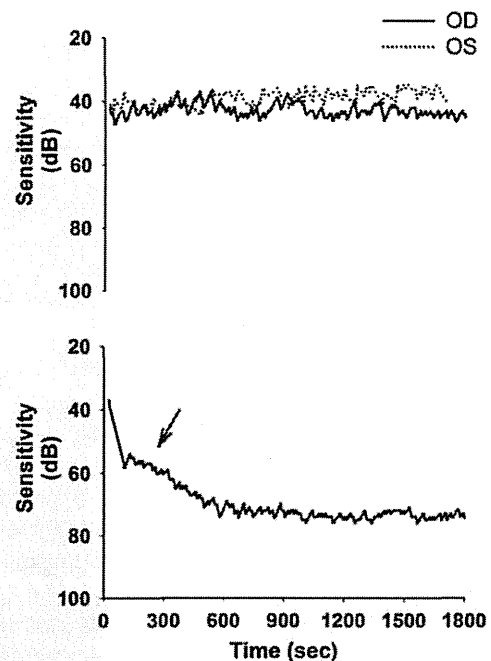


Fig. 3 Dark adaptometry curve of the patient (upper panel) shows a monophasic pattern without the characteristic decline attributed to rod function (arrow) that is seen in normal individuals (lower panel)

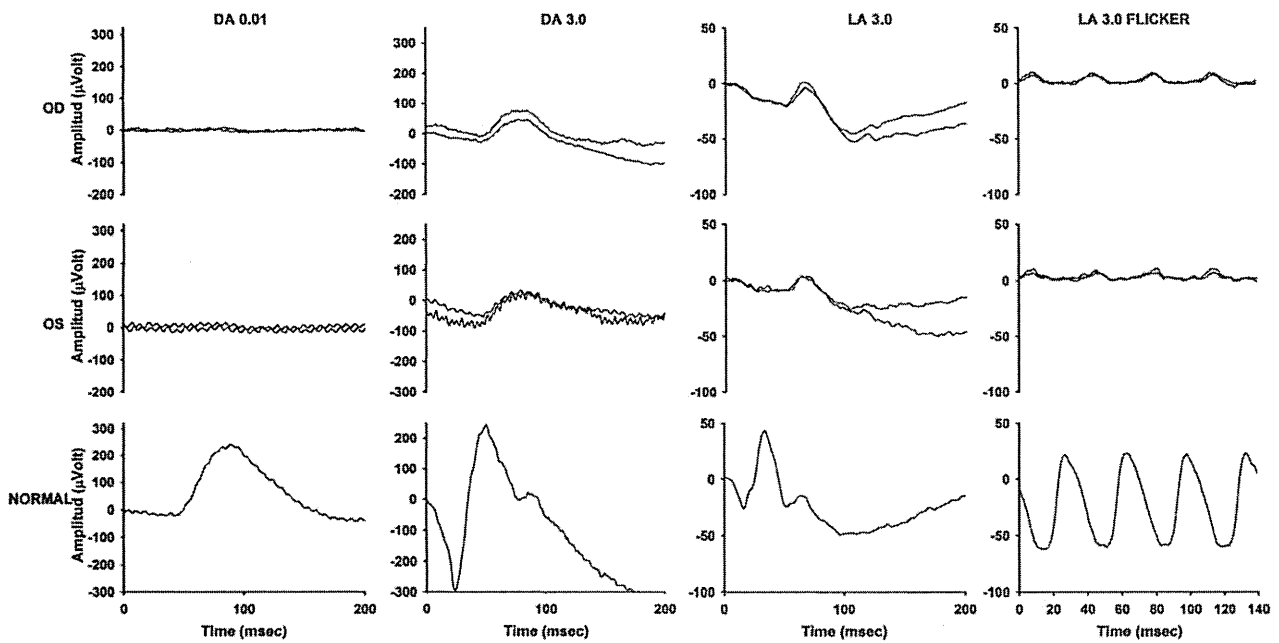


Fig. 4 Full-field electroretinograms (ERGs) of the patient and a normal subject. In the patient, there is no scotopic response (DA 0.01); the waveforms of the combined (DA 3.0) and photopic (LA 3.0) ERGs are very similar. The photopic ERG a- and b-waves are delayed

almost 20 ms when compared to the normal subject. Delayed 30-Hz flicker ERG (LA 3.0 flicker), with lower amplitude than the single-flash photopic a-wave are also detected

domain (DBD), which consists of 84 amino acids (cysteine 47 to valine 130) (Fig. 7). No other nucleotide substitution was detected in the patient. The cysteine residue at position 83 (Cys83) within the second zinc finger motif of the DBD (arrow) is conserved among orthologs of other vertebrate species (Fig. 7), predicting a functionally important amino acid residue.

The patient’s parents were heterozygotes for the mutation (p.C83Y). This mutation was not found in the 100 normal controls or in database searches of PubMed, The Human Gene Mutation Database (URL: <http://www.hgmd.cf.ac.uk/>), and of the Leiden Open Variation Database (<http://www.lovd.nl/>) [20].

Discussion

In this study, we describe the clinical, electrophysiological, and psychophysical findings of a 25-year-old male patient who was diagnosed with ESCS. Genetic analysis revealed a novel homozygous *NR2E3* mutation (p.C83Y). This is the first report of an ESCS patient with any *NR2E3* mutation in the Portuguese population.

The DBD of *NR2E3* is composed of highly conserved two zinc finger motifs that facilitate binding to target DNA sites [19]. Four cysteine residues are coordinated with one zinc atom in each zinc finger. Cys83 is the first cysteine residue of the second zinc finger (Cys83 to Cys103) [19].

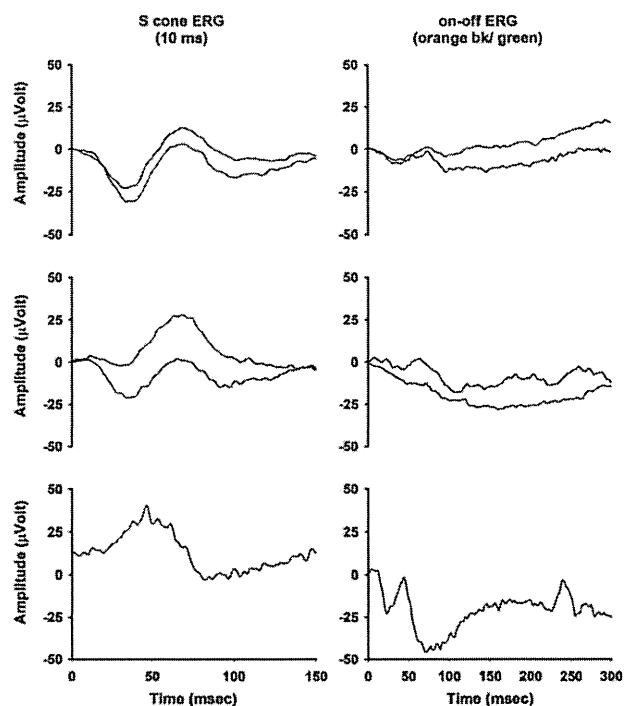
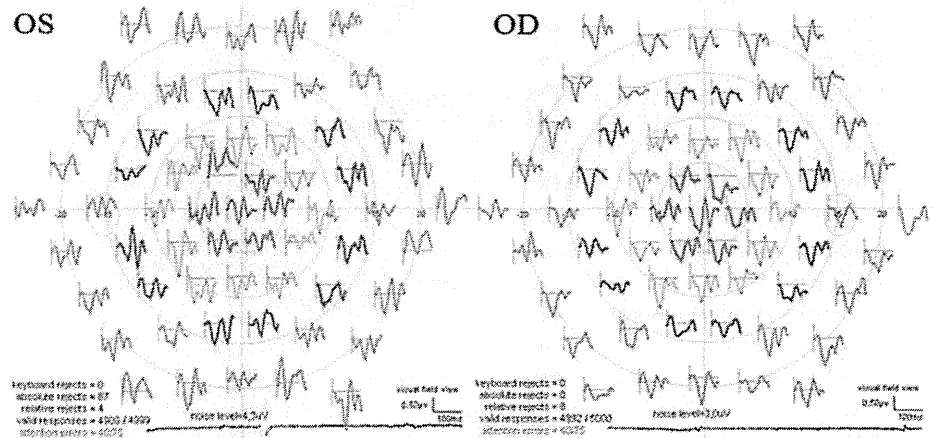


Fig. 5 Electroretinograms of specific chromatic stimulation. S-cone ERGs were delayed, simplified, and resemble the single flash cone ERGs. The ON-OFF responses with 200-ms orange stimulation are markedly decreased. The S-cone ERGs waveforms were not superimposable due to limited patient compliance

Fig. 6 Multifocal ERG. The analysis of the central response and four concentric rings are shown in **a**. Amplitudes and implicit time are compared with a database of normal subjects in **b**. There is an increase in the latency and a decrease in the amplitude of the N1 and P1 components in all the analyzed responses, even in the most central (Z1)



	Amplitude (nV/dg ²)			Implicit time (msec)		
	OD	OS	Normal	OD	OS	Normal
N₁						
Z ₁	57.6	34.4	102.4 ± 29.5	35.8	40.1	23.7 ± 1.6
Z ₂	41.8	15.7	53.4 ± 10.7	34.1	37.7	23.5 ± 1.1
Z ₃	31.5	30.9	37.7 ± 7.2	37.4	36.4	22.9 ± 1.1
Z ₄	18.5	18.9	28.3 ± 5.5	40.1	38.0	22.8 ± 1.2
Z ₅	15.9	11.7	22 ± 4.4	41.0	39.0	23.1 ± 1.2
P₁						
Z ₁	79.6	56.1	165.0 ± 40.0	54.6	56.9	46.4 ± 2.4
Z ₂	40.9	32.2	100.1 ± 18.6	54.9	57.2	42.5 ± 1.3
Z ₃	34.1	29.7	69.3 ± 13.0	58.2	57.7	41.1 ± 1.4
Z ₄	20.7	20.4	52.4 ± 10.6	62.9	58.3	40.4 ± 1.4
Z ₅	15.9	14.2	41.3 ± 9.0	63.6	64.1	40.6 ± 1.5

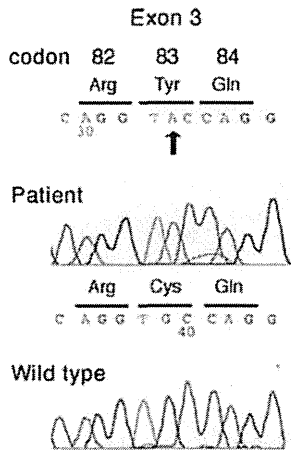


Fig. 7 **a** Partial nucleotide sequences of exon 3 in a wild-type and in the patient. A homozygous variation c.248G>A (exon 3) is shown in the patient (arrow), resulting in a new homozygous missense mutation (Cys83Tyr) in the DNA-binding domain of NR2E3 protein. **b** Amino acid alignment of the DNA binding domain of the human NR2E3 protein. The cysteine residue at position 83 within the second zinc finger motif (arrow) is highly conserved among orthologs of human NR2E3. hs: *Homo sapiens* (human); mm: *Mus musculus* (mouse); gg: *Gallus gallus* (chicken); xt: *Xenopus tropicalis* (xenopus); dr: *Danio rerio* (zebrafish)

The D-box, a short loop with six amino acid residues between the first cysteine (Cys83) and second cysteine (Cys90) of the second zinc finger [5], is important for homodimerization of NR2E3 to be functionally active, suggesting that Cys83 is an important amino acid. In vitro experiments using electrophoretic mobility shift assay showed that varied NR2E3 proteins with mutations in the zinc finger motifs exhibited reduced binding to the target DNA sites [28, 29]. Those NR2E3 mutant proteins, which were localized at least partially in cell nuclei, exhibited reduced transcriptional activity of the target gene [28, 29] and impaired dimerization [29] using cultured cells. The p. C83Y mutated NR2E3 protein is not able to dimerize to become active. This results in disruption of the target DNA binding sites leading to a null function of the DBD. It is expected that the homozygous p.C83Y mutation causes severe non-functional behavior of NR2E3 protein.

ESC'S shares several clinical features with GFS that is characterized by night blindness, pigmentary degeneration, macular and peripheral retinoschisis, posterior subcapsular cataract, markedly abnormal ERG and degenerative vitreous changes [30, 31]. Jacobson et al. demonstrated enhanced S-cone responses in patients with GFS [3], while NR2E3 mutations have been also found in GFS patients. Based on these findings, it was concluded that these two diseases are

likely to be one clinical entity [11], with two identifiable phenotypes in a wide-range spectrum of clinical expression of the same retinal degeneration [16, 20]. However, the absence of peripheral retinoschisis, posterior subcapsular cataract, and degenerative vitreous changes differentiates ESCS patients from patients with GFS phenotype. Our patient did not exhibit peripheral retinoschisis, cataract, or degenerative vitreous changes. The SD-OCT images revealed macular schisis with cystoid changes (Fig. 1), which are frequently seen in both ESCS and GFS [11, 16, 24] but are different from cystoid macular edema secondary to other conditions such as diabetic retinopathy and retinal vein occlusion that are characterized by the presence of leakage on fluorescein angiography.

The main ERG characteristics in our patient included the pathognomonic changes previously described in [24]. This included an absent rod ERG consistent with absence of rods. There was a simplified and delayed waveform to a standard flash under photopic and scotopic conditions, presumably both dominated by short-wavelength sensitive cones. The 30-Hz flicker ERG was severely abnormal and delayed and was smaller than the single flash cone ERG a-wave; these distinctive findings may be explained by considering the low temporal resolution of the S-cone system.

These results are in accordance with the histopathological studies that have demonstrated the absence of rods and the predominance of S-cone opsin over L/M cones in postmortem retinas of ESCS patients [32, 33]. Mild phenotypes of ESCS associated with compound heterozygous mutations have been found to have a residual rod response or a morphologically normal waveform of the combined ERG, either alone or together [15, 34]. Regarding the mfERG findings, Marmor et al. [35] previously described a normal waveform in the most central ring and a marked deterioration in the two paracentral rings in a patient with ESCS. Subsequently, similar mfERG findings have been described in five patients with ESCS, at least two of which had macular cysts [24]. Thus most of the patients had nearly normal central response [24, 35], suggesting preserved function of the most central macula retina in ESCS. However, our patient showed reduced amplitudes with delayed implicit times in both N1 and P1 components even in the most central ring (Z1) of both eyes (Fig. 6). The disorganization of laminar structure, namely macular schisis with cystoid changes (Fig. 1) can explain the reduced amplitudes of all the ring of the mfERG (Fig. 6). The condition of our patient with the homozygous p.C83Y mutation, causing expression of the putative non-functional NR2E3 protein, may be associated with a severer phenotype of ESCS that has reduced central mfERG responses compared with that of ESCS with preserved central responses.

In summary, we reported the first Portuguese ESCS patient with a novel homozygous mutation (p.C83Y) in the NR2E3 gene. The mutation, which resides within the

second zinc finger of the DBD, may cause a typical form of ESCS with nondetectable rod responses and reduced mfERG amplitudes in all eccentricities.

Acknowledgments This work was supported by grants from the Sociedade Portuguesa de Oftalmologia, from the Ministry of Education, Culture, Sports, Science and Technology of Japan [Grant-in-Aid for Scientific Research (C) #19592042] (TH) and the Vehicle Racing Commemorative Foundation (TH and HT).

References

- Marmor MF, Jacobson SG, Foerster MH, Kellner U, Weleber RG (1990) Diagnostic clinical findings of a new syndrome with night blindness, maculopathy, and enhanced S-cone sensitivity. *Am J Ophthalmol* 110:124–134
- Jacobson SG, Marmor MF, Kemp CM, Knighton RW (1990) SWS (blue) cone hypersensitivity in a newly identified retinal degeneration. *Invest Ophthalmol Vis Sci* 31:827–838
- Jacobson SG, Roman AJ, Roman MI, Gass JD, Parker JA (1991) Relatively enhanced S-cone function in the Goldmann-Favre syndrome. *Am J Ophthalmol* 111:446–453
- Haider NB, Jacobson SG, Cideciyan AV, Swiderski R, Streb LM, Searby C, Beck G, Hockey R, Hanna DB, Gorman S, Duhl D, Carmi R, Bennett J, Weleber RG, Fishman GA, Wright AF, Stone EM, Sheffield VC (2000) Mutation of a nuclear receptor gene, NR2E3, causes enhanced S-cone syndrome, a disorder of retinal cell fate. *Nat Genet* 24:127–131
- Kobayashi M, Takezawa S, Hara K, Yu RT, Umesono Y, Agata K, Taniwaki M, Yasuda K, Umesono K (1999) Identification of a photoreceptor cell-specific nuclear receptor. *Proc Natl Acad Sci USA* 96:4814–4819
- Haider NB, Naggert JK, Nishina PM (2001) Excess cone cell proliferation due to lack of a functional NR2E3 causes retinal dysplasia and degeneration in rd7/rd7 mice. *Hum Mol Genet* 10:1619–1626
- Cheng H, Khanna H, Oh EC, Hicks D, Mitton KP, Swaroop A (2004) Photoreceptor-specific nuclear receptor NR2E3 functions as a transcriptional activator in rod photoreceptors. *Hum Mol Genet* 13:1563–1575. doi:10.1093/hmg/ddl173
- Peng GH, Ahmad O, Ahmad F, Liu J, Chen S (2005) The photoreceptor-specific nuclear receptor Nr2e3 interacts with Crx and exerts opposing effects on the transcription of rod versus cone genes. *Hum Mol Genet* 14:747–764
- Cheng H, Aleman TS, Cideciyan AV, Khanna R, Jacobson SG, Swaroop A (2006) In vivo function of the orphan nuclear receptor NR2E3 in establishing photoreceptor identity during mammalian retinal development. *Hum Mol Genet* 15:2588–2602. doi:10.1093/hmg/ddl185
- Haider NB, Demarco P, Nystuen AM, Huang X, Smith RS, McCall MA, Naggert JK, Nishina PM (2006) The transcription factor Nr2e3 functions in retinal progenitors to suppress cone cell generation. *Vis Neurosci* 23:917–929
- Sharon D, Sandberg MA, Caruso RC, Berson EL, Dryja TP (2003) Shared mutations in NR2E3 in enhanced S-cone syndrome, Goldmann-Favre syndrome, and many cases of clumped pigmentary retinal degeneration. *Arch Ophthalmol* 121:1316–1323
- Nakamura Y, Hayashi T, Kozaki K, Kubo A, Omoto S, Watanabe A, Toda K, Takeuchi T, Gekka T, Kitahara K (2004) Enhanced S-cone syndrome in a Japanese family with a nonsense NR2E3 mutation (Q350X). *Acta Ophthalmol Scand* 82:616–622
- Nakamura M, Hotta Y, Piao CH, Kondo M, Terasaki H, Miyake Y (2002) Enhanced S-cone syndrome with subfoveal neovascularization. *Am J Ophthalmol* 133:575–577

14. Wright AF, Reddick AC, Schwartz SB, Ferguson JS, Aleman TS, Kellner U, Jurklics B, Schuster A, Zrenner E, Wissinger B, Lennon A, Shu X, Cideciyan AV, Stone EM, Jacobson SG, Swaroop A (2004) Mutation analysis of NR2E3 and NRL genes in enhanced S-cone syndrome. *Hum Mutat* 24:439
15. Hayashi T, Gekka T, Goto-Omoto S, Takeuchi T, Kubo A, Kitahara K (2005) Novel NR2E3 mutations (R104Q, R334G) associated with a mild form of enhanced S-cone syndrome demonstrate compound heterozygosity. *Ophthalmology* 112:2115
16. Pachydaki SI, Klaver CC, Barbazetto IA, Roy MS, Gouras P, Allikmets R, Yannuzzi LA (2009) Phenotypic features of patients with NR2E3 mutations. *Arch Ophthalmol* 127:71–75. doi:10.1001/archophthalmol.2008.534
17. Escher P, Gouras P, Roduit R, Tiab L, Bolay S, Delarive T, Chen S, Tsai CC, Hayashi M, Zernant J, Merriam JE, Mermod N, Allikmets R, Munier FL, Schorderet DF (2009) Mutations in NR2E3 can cause dominant or recessive retinal degenerations in the same family. *Hum Mutat* 30:342–351. doi:10.1002/humu.20858
18. Gerber S, Rozet JM, Takezawa SI, dos Santos LC, Lopes L, Gribouval O, Penet C, Peralut I, Ducroq D, Souied E, Jeanpierre M, Romana S, Frezal J, Ferraz F, Yu-Umesono R, Munnich A, Kaplan J (2000) The photoreceptor cell-specific nuclear receptor gene (PNR) accounts for retinitis pigmentosa in the Crypto-Jews from Portugal (Marranos), survivors from the Spanish Inquisition. *Hum Genet* 107:276–284
19. Coppeters F, Leroy BP, Beysen D, Hellemans J, De Bosscher K, Haegeman G, Robberecht K, Wuyts W, Coucke PJ, De Baere E (2007) Recurrent mutation in the first zinc finger of the orphan nuclear receptor NR2E3 causes autosomal dominant retinitis pigmentosa. *Am J Hum Genet* 81:147–157. doi:10.1086/518426
20. Schorderet DF, Escher P (2009) NR2E3 mutations in enhanced S-cone sensitivity syndrome (ESCS), Goldmann–Favre syndrome (GFS), clumped pigmentary retinal degeneration (CPRD), and retinitis pigmentosa (RP). *Hum Mutat* 30:1475–1485. doi:10.1002/humu.21096
21. Arden G, Gunduz K, Perry S (1988) Color vision testing with a computer graphics system: preliminary results. *Doc Ophthalmol* 69:167–174
22. Marmor MF, Fulton AB, Holder GE, Miyake Y, Brigell M, Bach M (2009) ISCEV Standard for full-field clinical electroretinography (2008 update). *Doc Ophthalmol* 118:69–77. doi:10.1007/s10633-008-9155-4
23. Arden G, Wolf J, Berninger T, Hogg CR, Tzekov R, Holder GE (1999) S-cone ERGs elicited by a simple technique in normals and in tritanopes. *Vision Res* 39:641–650
24. Audo I, Michaelides M, Robson AG, Hawlina M, Vaclavik V, Sandbach JM, Neveu MM, Hogg CR, Hunt DM, Moore AT, Bird AC, Webster AR, Holder GE (2008) Phenotypic variation in enhanced S-cone syndrome. *Invest Ophthalmol Vis Sci* 49:2082–2093. doi:10.1167/iov.05-1629
25. Khan NW, Jamison JA, Kemp JA, Sieving PA (2001) Analysis of photoreceptor function and inner retinal activity in juvenile X-linked retinoschisis. *Vision Res* 41:3931–3942
26. Brown M, Marmor M, Vaegan ZE, Brigell M, Bach M (2006) ISCEV Standard for Clinical Electro-oculography (EOG) 2006. *Doc Ophthalmol* 113:205–212. doi:10.1007/s10633-006-9030-0
27. Hood DC, Bach M, Brigell M, Keating D, Kondo M, Lyons JS, Palmowski-Wolfe AM (2008) ISCEV guidelines for clinical multifocal electroretinography (2007 edition). *Doc Ophthalmol* 116:1–11. doi:10.1007/s10633-007-9089-2
28. Kanda A, Swaroop A (2009) A comprehensive analysis of sequence variants and putative disease-causing mutations in photoreceptor-specific nuclear receptor NR2E3. *Mol Vis* 15:2174–2184
29. Roduit R, Escher P, Schorderet DF (2009) Mutations in the DNA-binding domain of NR2E3 affect in vivo dimerization and interaction with CRX. *PLoS One* 4:e7379. doi:10.1371/journal.pone.0007379
30. Peyman GA, Fishman GA, Sanders DR, Vlecek J (1977) Histopathology of Goldmann–Favre syndrome obtained by full-thickness eye-wall biopsy. *Ann Ophthalmol* 9:479–484
31. Nasr YG, Cherfan GM, Michels RG, Wilkinson CP (1990) Goldmann–Favre maculopathy. *Retina* 10:178–180
32. Ben-Arie-Weintrob Y, Berson EL, Dryja TP (2005) Histopathologic-genotypic correlations in retinitis pigmentosa and allied diseases. *Ophthalmic Genet* 26:91–100
33. Milam AH, Rose L, Cideciyan AV, Barakat MR, Tang WX, Gupta N, Aleman TS, Wright AF, Stone EM, Sheffield VC, Jacobson SG (2002) The nuclear receptor NR2E3 plays a role in human retinal photoreceptor differentiation and degeneration. *Proc Natl Acad Sci USA* 99:473–478
34. Lam BL, Goldberg JL, Hartley KL, Stone EM, Liu M (2007) Atypical mild enhanced S-cone syndrome with novel compound heterozygosity of the NR2E3 gene. *Am J Ophthalmol* 144:157–159. doi:10.1016/j.ajo.2007.03.012
35. Marmor MF, Tan F, Sutter EE, Bearse MA Jr (1999) Topography of cone electrophysiology in the enhanced S-cone syndrome. *Invest Ophthalmol Vis Sci* 40:1866–1873

厚生労働省 難病・がん等疾患分野の医療の実用化研究事業

次世代シーケンサーを用いたエクソーム配列解析による
黄斑ジストロフィーの原因遺伝子と発症機序の解明
(H23-実用化(難病) - 一般-006)

平成 25 年度 総合研究報告書

岩田 岳

平成 26 年 5 月

